



# Embryonal Tumors of the Central Nervous System<sup>1</sup>

Robert Y. Shih, LTC, MC, USA  
Kelly K. Koeller, MD

**Abbreviations:** ADC = apparent diffusion coefficient, AT/RT = atypical teratoid/rhabdoid tumor, CNS = central nervous system, CSF = cerebrospinal fluid, ETMR = embryonal tumor with multilayered rosettes, H-E = hematoxylin-eosin, NOS = not otherwise specified, PNET = primitive neuroectodermal tumor, WHO = World Health Organization

**RadioGraphics** 2018; 38:525–541  
<https://doi.org/10.1148/rg.2018170182>

**Content Codes:** **MR** **NR** **OI**

<sup>1</sup>From the Department of Neuroradiology, American Institute for Radiologic Pathology, Silver Spring, Md (R.Y.S., K.K.K.); Uniformed Services University of the Health Sciences, Bethesda, Md (R.Y.S.); Department of Radiology, Walter Reed National Military Medical Center, Bethesda, Md (R.Y.S.); and Department of Radiology, Mayo Clinic, 200 First St SW, Rochester, MN 55905 (K.K.K.). Received August 23, 2017; revision requested October 12 and received November 10; accepted November 20. For this journal-based SA-CME activity, the author K.K.K. has provided disclosures (see end of article); the other author, editor, and reviewers have disclosed no relevant relationships. **Address correspondence to** K.K.K. (e-mail: [koeller.kelly@mayo.edu](mailto:koeller.kelly@mayo.edu)).

Supported by the American Institute for Radiologic Pathology, the Joint Pathology Center, and Uniformed Services University of the Health Sciences. The views expressed in this article are those of the authors and do not necessarily reflect the official policy or position of the Department of Defense or the U.S. Government.

## SA-CME LEARNING OBJECTIVES

After completing this journal-based SA-CME activity, participants will be able to:

- List the radiologic-pathologic features of CNS embryonal tumors.
- Describe the new molecularly defined types/subtypes of CNS embryonal tumors.
- Discuss the increasing importance of molecular classification of CNS embryonal tumors.

See [www.rsna.org/education/search/RG](http://www.rsna.org/education/search/RG).

Embryonal tumors of the central nervous system (CNS) are highly malignant undifferentiated or poorly differentiated tumors of neuroepithelial origin and have been defined as a category in the World Health Organization (WHO) classification since the first edition of the “Blue Book” in 1979. This category has evolved over time to reflect our ever-improving understanding of tumor biology and behavior. With the most recent update in 2016, many previous histologic diagnoses incorporate molecular parameters for the first time (genetically defined entities). While medulloblastoma and atypical teratoid/rhabdoid tumor are familiar carryovers from the 2007 CNS WHO classification, there are major changes to the embryonal tumor category: for example, elimination of the term *CNS primitive neuroectodermal tumor* and addition of a new genetically defined entity, *embryonal tumor with multilayered rosettes, C19MC-altered*. The purpose of this article is to discuss both the radiologic-pathologic features of CNS embryonal tumors and the new molecularly defined types/subtypes that will become the standard classification/terminology for future diagnoses and tumor research.

## Introduction with Historical Perspectives

Embryonal tumors of the central nervous system (CNS) are highly malignant undifferentiated or poorly differentiated tumors of neuroepithelial origin and have been defined as a category in the World Health Organization (WHO) classification since the first edition of the “Blue Book” in 1979 (1). This category has evolved over time through the often contentious deliberation of expert neuropathologists to reflect our ever-improving understanding of tumor biology and behavior (1). For example, the second edition in 1993 added neuroblastoma/ganglioneuroblastoma, ependymoblastoma, and primitive neuroectodermal tumor (PNET) to join medulloblastoma and medulloepithelioma in the embryonal category while moving glioblastoma to the astrocytic category (1). The third edition in 2000 added atypical teratoid/rhabdoid tumor (AT/RT) and two histologic subtypes of medulloblastoma (desmoplastic and large cell) (1). The fourth edition in 2007 added two more histologic subtypes (extensively nodular and anaplastic) while renaming supratentorial PNET to CNS PNET as a heterogeneous group of extracerebellar embryonal tumors.

The 2007 WHO classification has served as the nosologic standard for tumors of the CNS for the past decade (2). According to that iteration, there are three types of embryonal tumors in the CNS: medulloblastoma, AT/RT, and CNS PNET. These also include four histologic subtypes/variants of medulloblastoma (desmoplastic/nodular, extensive nodularity, large cell, anaplastic) and four histologic subtypes/variants of CNS PNET (neuroblastoma, ganglioneuroblastoma, medulloepithelioma, ependymoblastoma). Because the

## TEACHING POINTS

- Embryonal tumors of the CNS have been defined as a category in the WHO classification since the first edition (1979). In the fourth edition (2007), the three types are medulloblastoma, atypical teratoid/rhabdoid tumor (AT/RT), and CNS primitive neuroectodermal tumor (PNET).
- A recent update to the fourth edition (2016) adds genetically defined subtypes of medulloblastoma, replaces the term *CNS PNET* with *CNS embryonal tumor, not otherwise specified*, and replaces ependymoblastoma with the genetically defined entity *embryonal tumor with multilayered rosettes* (ETMR).
- First described in 1924, medulloblastoma is the prototypical CNS embryonal tumor and accounts for nearly two-thirds of cases. While the classic description is a midline cerebellar mass in a child, about one-fourth of cases will be laterally positioned and one-fourth will manifest in adulthood.
- The relatively new entities AT/RT and ETMR were officially named in 1996 and 2010, respectively. They are less common and more aggressive and tend to affect the very young (age < 4 years). They are now genetically defined by loss of *INI1* expression and amplification of *C19MC*, respectively.
- There is significant overlap in the histologic and radiologic appearance of embryonal tumors. Their imaging features reflect their cellularity; therefore, this category should be considered for any tumor of the CNS in a young patient with high attenuation at CT and low signal intensity on T2-weighted images/ADC maps.

WHO classifications for tumors of various organ systems have not released a fifth edition, a recent 2016 update (3) is considered a revised fourth edition, stating: "For the first time, the WHO classification of CNS tumors uses molecular parameters in addition to histology to define many tumor entities, thus formulating a concept for how CNS tumor diagnoses should be structured in the molecular era."

There are three major changes to embryonal tumors in the 2016 CNS WHO classification. First, on top of *medulloblastoma, not otherwise specified* (NOS) and the four histologically defined subtypes of medulloblastoma, there are now also four genetically defined subtypes of medulloblastoma based on the presence or absence of activation in the wingless integration (WNT) or sonic hedgehog (SHH) signaling pathways. Second, the term or subcategory of *primitive neuroectodermal tumor* has been removed from the lexicon and replaced by *CNS embryonal tumor, NOS* when there is no histologic evidence of primitive neural tube or neuronal differentiation to suggest either medulloepithelioma or CNS neuroblastoma/ganglioneuroblastoma. Third, the entity of ependymoblastoma, first described by Bailey and Cushing in 1926 and characterized by ependymoblastic rosettes (4), has been removed and replaced by the new entity *embryonal tumor with multilayered rosettes* (ETMR), which is characterized by amplification of a microRNA gene cluster

on chromosome 19. Important modifications between the 2007 and 2016 WHO classification schemes are summarized in the Table.

Because of this transition period, there is a need to be familiar with both the 2007 terminology, which serves as the basis for most of our existing diagnoses and recent literature, as well as the 2016 terminology. The purpose of this review article is to discuss both the radiologic-pathologic features of CNS embryonal tumors and the new molecularly defined types or subtypes that will become the new standard for future diagnoses and tumor research. As a group, embryonal tumors are uncommon and account for 1% of all CNS tumors. As the name would suggest, these malignant tumors (WHO grade IV) tend to affect the young (median age, 9 years) and are the most common CNS tumor type in the first 4 years of life. After pilocytic astrocytoma and malignant glioma, they are the third most common in all children and adolescents (age 0–19 years), accounting for 11% of all CNS tumors in the first 2 decades. Nearly two-thirds of CNS embryonal tumors are diagnosed as medulloblastomas, followed distantly by AT/RT and then CNS PNET (5).

## Medulloblastoma: the Prototypical CNS Embryonal Tumor

Medulloblastoma is the most common CNS embryonal tumor and most common pediatric CNS malignancy (6). It accounts for 25% of all intracranial pediatric brain tumors and is second only to pilocytic astrocytoma as the most common pediatric brain tumor (7). The annual overall incidence is 1.8 cases per million, and the annual childhood incidence is 6 cases per million (8). In the United States, the highest incidence occurs in white non-Hispanics followed by Hispanics and African Americans (6). Nearly 25% of all medulloblastomas arise in adults (9). The mean age at diagnosis is 9 years with peaks at 3 and 7 years (10). Among those older than 3 years, males are more commonly affected (1.7:1), while there is no gender predilection for those younger than 3 years (11). Occasional familial cases and increased rates of cancer in first-degree relatives have been noted (7,12).

The tumor is most commonly located in the cerebellum (94%), particularly the vermis (>75%), and frequently grows into the fourth ventricle (Fig 1). A more lateral location in the cerebellar hemisphere may be seen in older children, adolescents, and adults (10,13,14) (Fig 2).

At initial medical evaluation, most patients with the tumor have had symptoms for less than 3 months (15,16). Common clinical manifestations reflect increased intracranial pressure and include headache, nausea, vomiting, and cerebel-

### Comparison of CNS Embryonal Tumor Category between 2007 and 2016 WHO Classifications

#### 2007 WHO classification

- Medulloblastoma
- Desmoplastic/nodular medulloblastoma
- Medulloblastoma with extensive nodularity
- Anaplastic medulloblastoma
- Large cell medulloblastoma
- Atypical teratoid/rhabdoid tumor (AT/RT)
- CNS primitive neuroectodermal tumor (PNET)\*
- Ependymoblastoma\*
- Medulloepithelioma
- CNS neuroblastoma
- CNS ganglioneuroblastoma

#### 2016 WHO classification

- Medulloblastoma, genetically defined<sup>†</sup>
- WNT-activated<sup>†</sup>
- SHH-activated and TP53-mutant<sup>†</sup>
- SHH-activated and TP53 wild-type<sup>†</sup>
- Non-WNT/non-SHH (group 3 and group 4)<sup>†</sup>
- Medulloblastoma, histologically defined
- Classic
- Desmoplastic/nodular
- With extensive nodularity
- Large cell/anaplastic
- Medulloblastoma, not otherwise specified (NOS)
- Atypical teratoid/rhabdoid tumor<sup>‡</sup>
- Embryonal tumor with multilayered rosettes (ETMR), C19MC-altered<sup>‡</sup>
- Medulloepithelioma
- CNS neuroblastoma
- CNS ganglioneuroblastoma
- CNS embryonal tumor, not otherwise specified<sup>†</sup>

\*Removed in 2016 WHO classification.

<sup>†</sup>Added since 2007 WHO classification.

<sup>‡</sup>Both AT/RT and ETMR are now defined by genetic/molecular alteration of INI1 or C19MC, respectively. In the absence of that feature, the morphologic diagnoses *CNS embryonal tumor with rhabdoid features* or *embryonal tumor with multilayered rosettes, NOS* are also available, when based on histologic findings alone.

lar ataxia. Cranial nerve palsies and long tract signs from brainstem compression are less common (6). Seizures are atypical but may herald the presence of metastatic disease (15). Papilledema (related to hydrocephalus), nystagmus, limb ataxia, and dysdiadochokinesia (particularly in lateral cerebellar hemisphere lesions) are commonly present at physical examination (15,16).

At gross pathologic analysis, medulloblastomas typically manifest as pink or gray friable masses that frequently fill the fourth ventricle (6). Those arising from the cerebellar hemispheres are usually firmer and more circumscribed, reflecting a tendency for the desmoplastic variant (6). Gross hem-

orrhage may occasionally occur (17). While small necrotic regions may be evident, extensive necrosis is rare (6). Discrete leptomeningeal nodules are common as evidence of dissemination (6).

### Medulloblastoma: Histopathologic Features versus Molecular Markers

All medulloblastomas are regarded by the WHO as grade IV neoplasms, with four major subtypes recognized on a histopathologic basis: classic, desmoplastic/nodular, extensively nodular, and large cell/anaplastic (6). Over several decades, a growing number of chromosomal abnormalities have been linked with medulloblastomas, the most common (30%–45%) being the loss of chromosomal arm 17p (18,19). On the basis of transcriptome or methylome profiling, subsequent investigations identified several molecular clusters of medulloblastomas that have demonstrated increased clinical utility and a higher degree of correlation with prognosis than achieved with histopathologic analysis alone (6). By consensus, these clusters have been categorized into four distinct groups based on activation of their signal transduction pathways: WNT-activated (~10% of medulloblastomas), SHH-activated (~30%), group 3 (~20%), and group 4 (~40%), the latter two of which do not show activation of either SHH or WNT cell signaling pathways and are regarded (for the time being) as provisional variants, as they are not as well separated by current laboratory assays (6,20). These four molecular groups based on their signaling transduction pathways have their own associations with clinical, demographic, prognostic, and (to some extent) imaging features.

The SHH signaling pathway is believed to be a driver of tumor initiation (21,22). Medulloblastomas arising from this signal transduction pathway have equal sex prevalence and are believed to arise from cerebellar granule neuron cell precursors of the external granular cell layer, cochlear nucleus, and possible neural stem cells of the subventricular zone (6,22). They most commonly occur in the cerebellar vermis and hemispheres (22,23). TP53-mutant tumors occur more commonly in children, correlate with the large cell/anaplastic medulloblastoma variant, and are frequently associated with chromosome 17p loss and amplification of MYCN and GLI2. TP53 wild-type tumors are more common in both infancy (<4 years of age) and adolescence/young adulthood (>16 years old), correlate with the desmoplastic/nodular variant, and are associated with chromosome 10q loss, PTCH1 deletion (seen in basal cell nevus or Gorlin syndrome), and numerous other genetic mutations (6,22). SHH-activated TP53-mutant tumors commonly

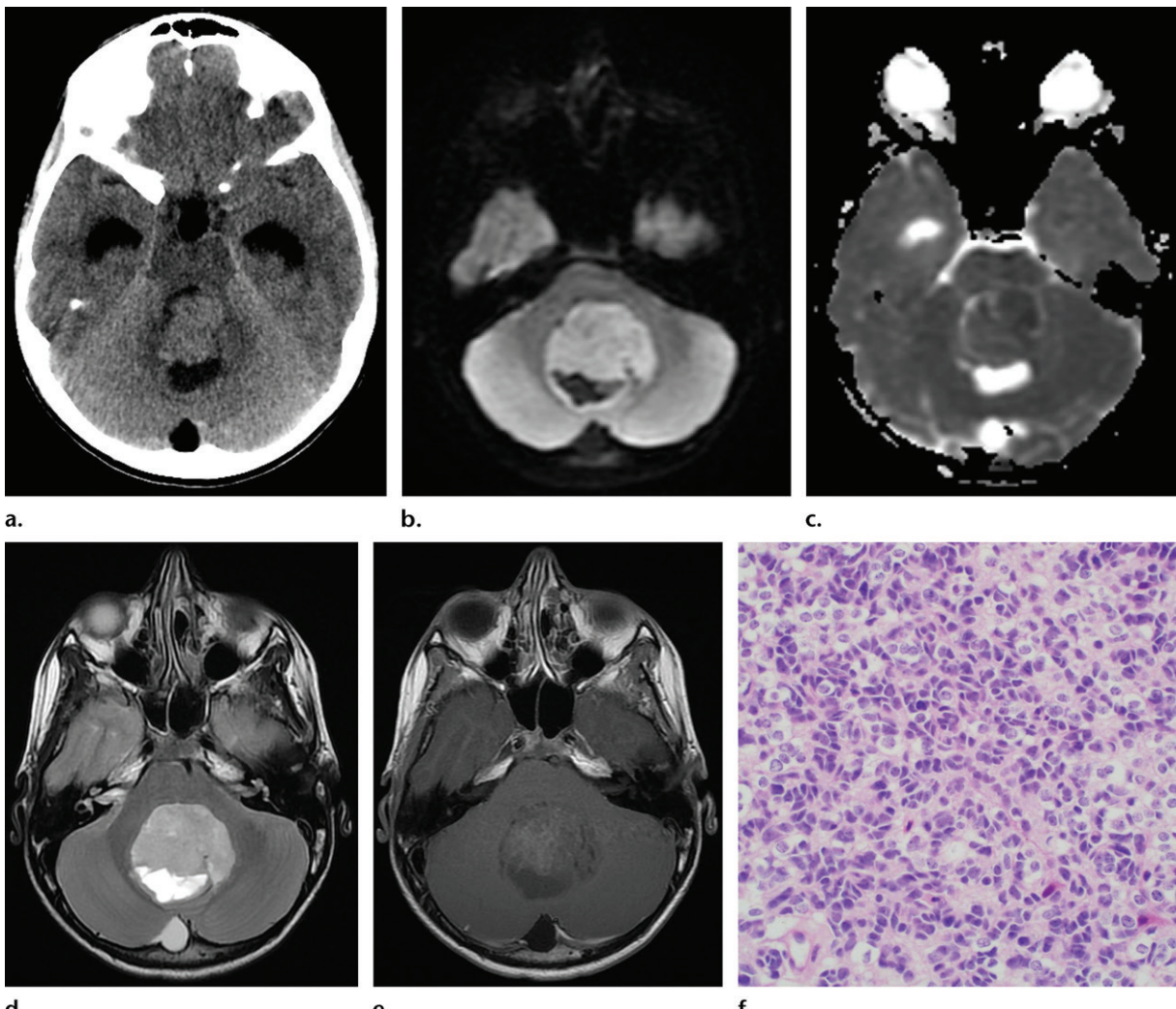


**Figure 1.** Medulloblastoma, classic (histologically defined), in a 12-year-old boy with headache/nausea for 1 month and vomiting/torticollis for 3–5 days. (a) Axial head computed tomographic (CT) image shows obstructive hydrocephalus caused by a hyperattenuating mass in the midline posterior fossa. A small arachnoid cyst next to the midline occipital bone is incidentally noted. (b, c) Axial diffusion-weighted image (b) and apparent diffusion coefficient (ADC) map (c) show restricted diffusion in the solid portion of the tumor, with free diffusion in the cystic portion. (d, e) Axial T2-weighted (d) and postcontrast T1-weighted (e) magnetic resonance (MR) images show well-defined margins, minimal vasogenic edema, and subtle enhancement. (f) Low-power photomicrograph shows a highly cellular neoplasm composed of small blue cells with pleomorphic nuclei (round vs carrot-shaped), consistent with an embryonal tumor and correlating with the CT and diffusion-weighted imaging findings. (Hematoxylin-eosin [H-E] stain.) The patient underwent suboccipital craniotomy for gross total resection of the cerebellar tumor. (Results of screening MR imaging of the spine and lumbar puncture for cerebrospinal fluid [CSF] dissemination were both negative.)

manifest evidence of dissemination through the neuraxis at presentation (22). The prognosis is extremely variable: poor (41% 5-year survival) for those with *TP53*-mutant tumors compared with better outcome (76% 5-year survival) for those with *TP53* wild-type tumors (6,22).

WNT-activated medulloblastoma is associated with a striking long-term survival rate (near 100%) with standard therapy (6). Among genetic markers, somatic mutations involving *CTNNB1* (which encodes β-catenin) are the most common (90%) (24), and nearly all show monosomy 6 (6,21). Unlike the overall male predominance and typical cerebellar origin seen in most medulloblastomas, those related to WNT pathways

show a female predominance (2:1) and are more associated with a dorsal brainstem site of origin (believed to arise from lower rhombic lip progenitor cells). Accordingly, these tumors frequently manifest as fourth ventricle masses at imaging (6). Given the excellent survival rate of patients with these tumors, it may be possible to implement less aggressive therapy (21). Rarely, tumors with this activation pathway may be associated with Turcot syndrome (21).

The remaining medulloblastomas do not show activation of either SHH or WNT signaling pathways (non-SHH/non-WNT) and are not as well defined or understood as medulloblastomas related to those pathways. As currently regarded

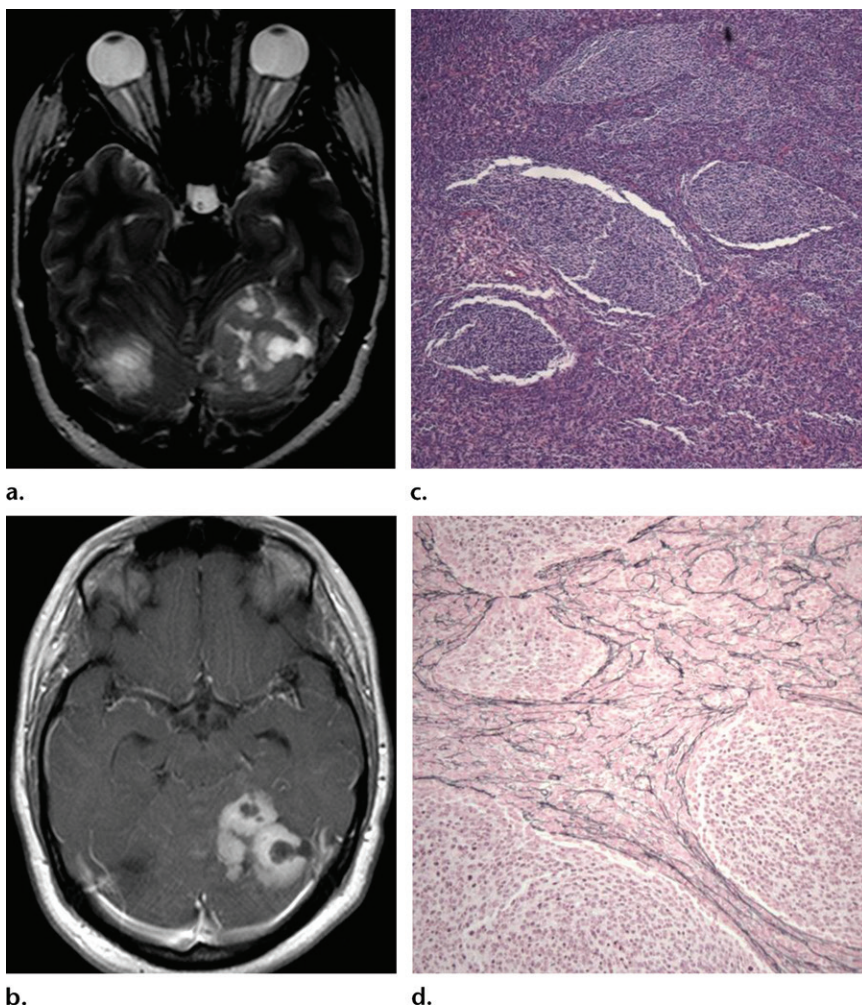


**Figure 2.** Medulloblastoma, desmoplastic/nodular (histologically defined), in a 27-year-old woman with headaches and gait instability for 1 month. (a, b) Axial T2-weighted (a) and postcontrast T1-weighted (b) images show a larger mass with heterogeneous enhancement in the left superior cerebellum and a smaller mass without enhancement in the right superior cerebellum. There is also bilateral papilledema without obstructive hydrocephalus. The patient underwent biopsy and debulking of the left-sided lesion. (c) Low-power photomicrograph shows a densely packed small round blue cell tumor, with relatively pale nodules of more-differentiated neuronal cells embedded in a stroma containing less-differentiated embryonal cells. (H-E stain.) (d) Low-power photomicrograph from reticulin immunohistochemistry shows that the nodules are reticulin poor while the stroma is reticulin rich (black staining). Lateral medulloblastomas can be seen at all ages but are more common in young adults, often with desmoplastic/nodular histologic features (SHH-activated).

provisional variants, they are generically divided into group 3 and group 4 medulloblastomas. Group 3 tumors comprise about 20% of all medulloblastomas. They are most common during infancy and childhood and show a 2:1 male predominance (6,25). Most group 3 tumors correspond to the classic histologic pattern (6,21). Other gene mutations (*MYC* amplification, *PVT1-MYC* and *GLI1/GLI1B* structural variants, and isochromosome 17q) are common (6). The tumors are believed to arise from CD133+/lineage-neural stem cells with possible contribution from cerebellar granule neuron cell precursors of the external granular cell layer (6). *MYC* family amplification is associated with higher clinical risk, and many patients with these tumors (40%) show evidence of metastatic spread at presentation (26). Not surprisingly, tumors of this group carry the worst prognosis among the four molecular groups of medulloblastoma (21).

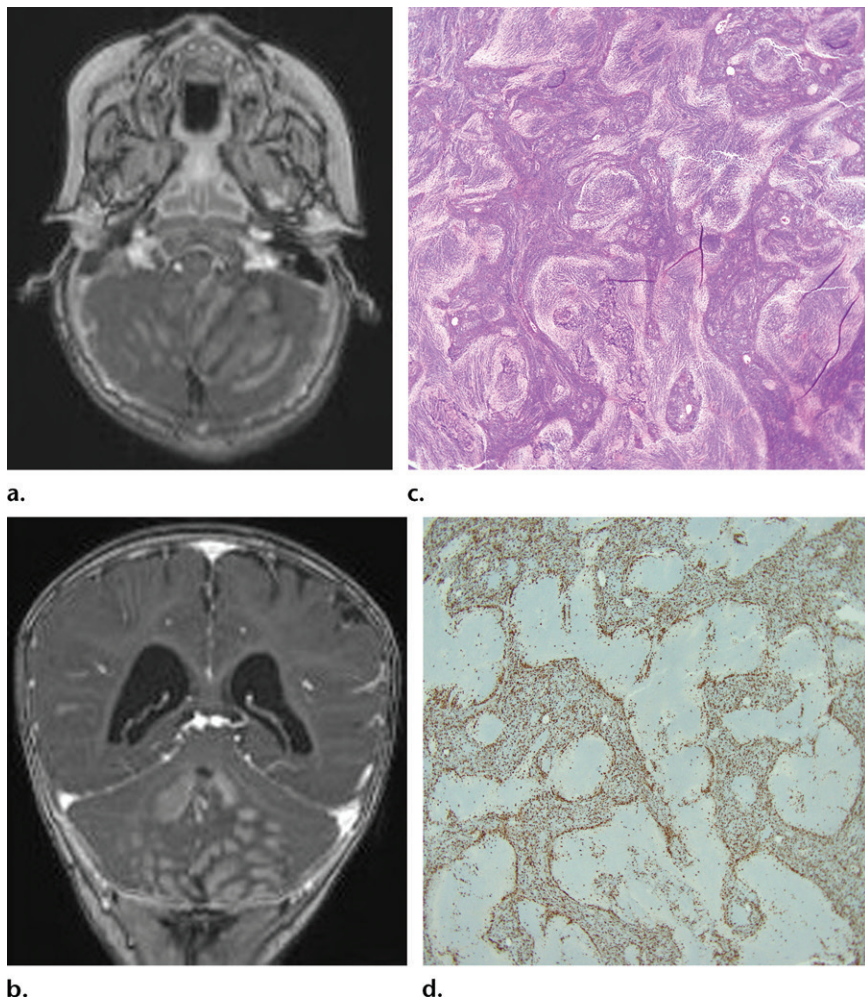
Group 4 medulloblastomas comprise the largest single group (40%), are seen at all ages (peak prevalence at 5–15 years) with a 3:1 male predominance, and conform to the classic histopathologic pattern (6,25). A putative cell of

origin remains unknown (6). Genetic alterations include *MYCN* amplification, isochromosome 17q (seen in 66%), and loss of X chromosome in 80% of females (6,21). In general, patients with these tumors have an intermediate prognosis, similar to those with SHH-activated *TP53* wild-type medulloblastomas (21).

Among the histopathologic subtypes, classic medulloblastoma is predominantly seen in childhood and is the most common overall (72%), with an archetypal CNS small blue cell tumor pattern defined by a sheet-like arrangement of densely packed undifferentiated embryonal cells with numerous mitotic figures, apoptotic bodies, and Homer-Wright rosettes (27). This subtype is less common in infants and adults (27). Medulloblastomas with classic histopathologic features strongly correlate with WNT-activated medulloblastoma.

The desmoplastic/nodular subtype accounts for about 20% of all medulloblastomas but about 50% of those occurring in children younger than 3 years. It predominates in the cerebellar hemispheres, and most medulloblastomas arising in the cerebellar hemispheres are of this subtype. Less

**Figure 3.** Medulloblastoma with extensive nodularity (histologically defined) in a 9-month-old girl with increasing head circumference at routine physical examination (otherwise asymptomatic). (a, b) Axial (a) and coronal (b) postcontrast T1-weighted images show a large nodular grape-like enhancing mass, midline and centered at the cerebellar vermis, producing chronic hydrocephalus with mild ventriculomegaly. (c) Low-power photomicrograph shows more extensive nodularity compared with that in Figure 2c. These nodules contain more-differentiated neuronal cells and are therefore relatively pale (lower cellularity). (H-E stain.) (d) Low-power photomicrograph from Ki-67 immunohistochemistry shows low mitotic activity in the nodules (minimal staining) with high mitotic activity in the background stroma (prominent staining). Medulloblastoma with extensive nodularity usually manifests in infancy and along with the desmoplastic/nodular subtype also tends to have a better overall prognosis.



commonly, it arises in the midline. It is associated with a more favorable prognosis in young children, causing less frequent metastatic disease compared with other medulloblastoma subtypes. In most cases, treatment may be limited to surgical resection and chemotherapy without use of radiation therapy (28). At histopathologic analysis, it is characterized by nodular reticulin-free zones ("pale islands") surrounded by a dense reticulin network of poorly differentiated cells (29). Children with *SUFU*-related basal cell nevus (Gorlin) syndrome have a 20 times increased risk of developing a desmoplastic medulloblastoma (29). MR imaging surveillance and genetic counseling for family members are highly recommended in these cases (29). Desmoplastic/nodular medulloblastoma is associated with SHH-activated tumors that also show *TP53* wild type (29).

The medulloblastoma with extensive nodularity (MBEN) subtype accounts for about 3%–4% of all medulloblastomas. Similar to the desmoplastic/nodular subtype, it is much more common in children younger than 3 years (20% of cases) and is associated with a favorable outcome (up to 95% survival at 8 years) using current therapeutic regi-

mens, even in the presence of metastatic disease (30,31). The MR imaging appearance is characteristic, with a large multinodular mass in a grape-like cluster centered in the vermis (>80%) and occasionally involving the cerebellar hemispheres (30) (Fig 3). Rarely, a gyriform pattern of contrast enhancement involving the cerebellar folia may be seen (32,33). Histopathologically, it overlaps in many features with the desmoplastic/nodular subtype and also involves SHH activation and *SUFU* mutations (30). Reticulin-free zones are unusually enlarged compared with those seen in the desmoplastic/nodular subtype. An even stronger association with basal cell nevus syndrome than seen in desmoplastic/nodular medulloblastoma warrants MR imaging surveillance and familial genetic counseling (30).

Large cell medulloblastoma and anaplastic medulloblastoma were considered separate entities in the 2007 WHO classification but are now regarded as a single category, since nearly all large cell tumors show an anaplastic component and both are associated with a poor prognosis (6,31,34). Large cell/anaplastic medulloblastoma accounts for about 10% of all medulloblastomas

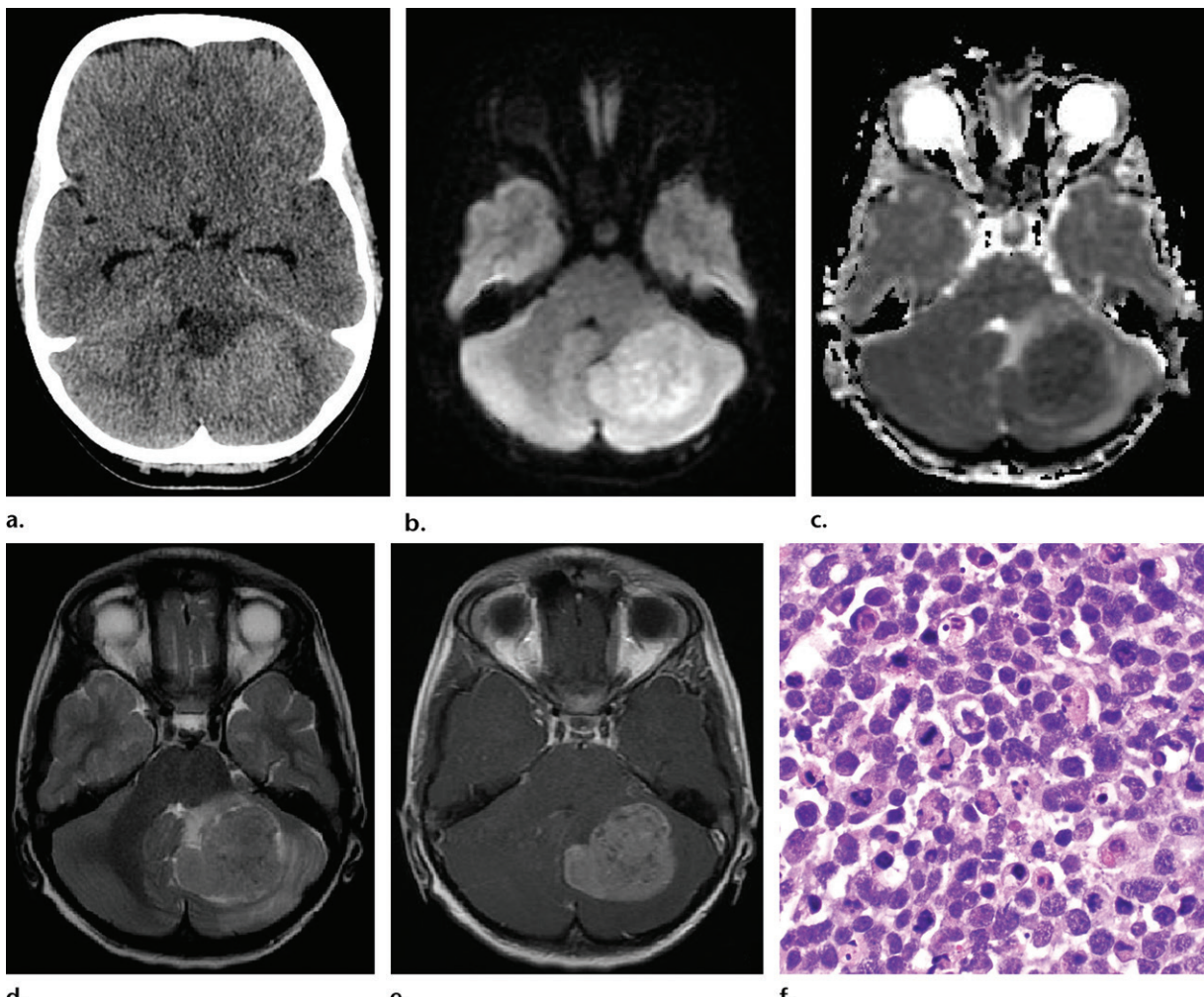


**Figure 4.** Medulloblastoma, large cell/anaplastic (histologically defined), in an 8-year-old boy with early morning headaches, nausea, and vomiting for 2 weeks. **(a)** Axial head CT image shows a large hyperattenuating mass in the left cerebellar hemisphere without obstructive hydrocephalus. **(b, c)** Axial diffusion-weighted image (**b**) and ADC map (**c**) show corresponding restricted diffusion, consistent with a highly cellular tumor. **(d, e)** Axial T2-weighted (**d**) and postcontrast T1-weighted (**e**) images show a heterogeneously enhancing mass with well-defined margins and mild adjacent vasogenic edema. **(f)** High-power photomicrograph shows anaplastic features with a marked degree of nuclear enlargement, pleomorphism, and molding/wrapping. This has been called a “starry sky” appearance and bears some resemblance to the appearance of large cell lymphoma. (H-E stain.) Large cell/anaplastic is the most aggressive medulloblastoma subtype and tends to have the worst overall prognosis of the four histologically defined subtypes.

over the entire age spectrum (35). Severe anaplasia, marked nuclear pleomorphism, abundant mitotic activity, and apoptosis are seen at histopathologic analysis (35) (Fig 4). This subtype is nearly always seen among group 3 or SHH-activated medulloblastomas and represents a group of high-risk tumors carrying the worst prognosis and requiring intensive adjuvant therapy (35). The 5-year progression-free survival is 30%–40%. Those that have SHH activation with *TP53* mutation and group 3 tumors with *MYC* amplification are even more aggressive (35).

Surgical resection, chemotherapy, and radiation therapy are the cornerstones of treatment of medulloblastomas. Intensified local therapy directed to the posterior fossa is recommended as initial treatment of SHH medulloblastoma, while a modified approach focused on metastatic

disease is advocated for group 3 and 4 tumors, as this is the most common cause of death in these subtypes (36). Remarkable progress in the prognosis of affected patients has been achieved, with 5-year survival rates now frequently exceeding 85%. However, avoiding long-term toxic effects is challenging. Radiation therapy is generally not used in younger children to avoid deleterious impacts on early brain development (37,38).

### Medulloblastoma: Imaging Features

Imaging manifestations of the tumor are characteristic and, when combined with clinical features, highly suggestive of the diagnosis although not necessarily pathognomonic. At CT, a hyperattenuating well-defined enhancing mass located in the cerebellar vermis with surrounding edema and frequent hydrocephalus is the classic appearance, but

variability is common (40%), frequently from cyst formation and calcification (17). As with virtually all brain tumors, MR imaging is superior to CT in depiction of medulloblastomas and is considered the reference standard for imaging.

Typical sequence acquisitions include sagittal and axial T1-weighted, axial (and optional coronal) fluid-attenuated inversion-recovery (FLAIR)/T2-weighted, diffusion-weighted, gradient-echo/susceptibility-weighted, and postcontrast T1-weighted imaging. Perfusion-weighted imaging, MR spectroscopy, and positron emission tomography (PET) may also be used, depending on the perspective of the performing radiologist. The combination of falcine or tentorial calcification and a presumptive medulloblastoma has been linked with basal cell nevus syndrome (39). Even more heterogeneity may be noted at MR imaging, with variable signal intensity on both T1- and T2-weighted images (17). Nearly all medulloblastomas demonstrate enhancement on postcontrast images (17).

Corresponding to hyperattenuation of the tumor at CT as a feature of hypercellularity, diffusion-weighted imaging shows restricted diffusion in medulloblastomas in the vast majority of cases. The ADC (ADC minimum [ $ADC_{min}$ ] or normalized ADC [ $nADC$ ]) in medulloblastomas typically ranges from  $0.54 \times 10^{-3}$  mm $^2$ /sec for  $ADC_{min}$  to  $0.70 \times 10^{-3}$  mm $^2$ /sec for  $nADC$  (40). In a separate study,  $ADC_{min}$  less than  $0.66 \times 10^{-3}$  mm $^2$ /sec was identified as a threshold that provided maximal accuracy (41). Using a higher  $b$  value at 3.0-T imaging has been reported to show improved contrast compared with normal tissue, allowing detection of additional less prominent lesions (42). Rarely, restricted diffusion may be absent in the tumor, perhaps reflecting a lack of reticulin architecture in certain subtypes at histopathologic analysis (43).

Although overlap is possible, certain imaging features may implicate particular medulloblastoma subtypes. Mean ADC and  $ADC_{min}$  have been noted to be lower in classic medulloblastomas compared with large cell/anaplastic tumors (44). Focal cysts are more common in the classic and desmoplastic subtypes, while leptomeningeal enhancement and ring enhancement are more common in the large cell/anaplastic subtype (44). Implementation of support vector machine-based classifiers using ADC histogram and textural features may provide further clarity in subtype discrimination in the future (45).

Elevated choline peaks, reduced N-acetyl-aspartate and creatine peaks, and occasional elevated lipid and lactic acid peaks are typical but not specific MR spectroscopic features of medulloblastomas, with improved accuracy in

differentiation from other posterior fossa tumors when at least two echo times are used (46). In most cases, fluorine 18 fluorodeoxyglucose PET shows uniform intense uptake throughout the tumor in a pattern similar to that of glioblastoma (47). Arterial spin-labeled perfusion imaging has shown significantly greater relative tumor blood flow and a wider range of variability in medulloblastoma compared with those in pilocytic astrocytoma, although correlation with specific histologic features is lacking (48). After treatment of medulloblastoma with radiochemotherapy, perfusion is significantly lower throughout the brain (49).

While foraminal extension from the fourth ventricle is uncommon, leptomeningeal spread from the craniospinal axis is common, reported to be as high as 33% (50) (Fig 5). Ideally, MR imaging of the spinal axis should be performed at the time of initial evaluation of the primary mass. Attempting to make this assessment after resection of the posterior fossa mass may be hindered by hemorrhagic debris within the thecal sac, making it difficult to confidently identify leptomeningeal deposits (51). The presence of such dissemination is an important therapeutic consideration, as it generally warrants modification of subsequent radiation therapy, with delivery of a boost dosage to this location (17). Distant metastatic disease is rare, with osseous and lymph node lesions most common and metastases to a wide variety of other sites much less common (6,17).

When the tumor arises in adolescents and adults, it is more commonly located in the cerebellar hemisphere, often as a poorly defined mass, frequently with cyst-like changes (17). Additional imaging features may allow suspicion for various subtypes of the disease, such as the striking grape-like nodularity typical of medulloblastoma with extensive nodularity (17). A mass involving the cerebellar hemisphere with extension to the overlying meninges, occasionally with leptomeningeal enhancement, should raise concern for the desmoplastic/nodular subtype and may mimic the appearance of a meningioma (17). Large cell/anaplastic medulloblastomas commonly show cysts, regions of necrosis, and hemorrhage.

Recurrence of disease is common, usually arising in the first 2 years of initial treatment and manifesting as leptomeningeal dissemination or focal nodular enhancement in the posterior fossa (17). With the addition of molecular marker data, greater accuracy in assessing risk of recurrence is emerging. SHH medulloblastoma tends to recur locally, while group 3 and 4 tumors have greater propensity for metastatic spread (36).

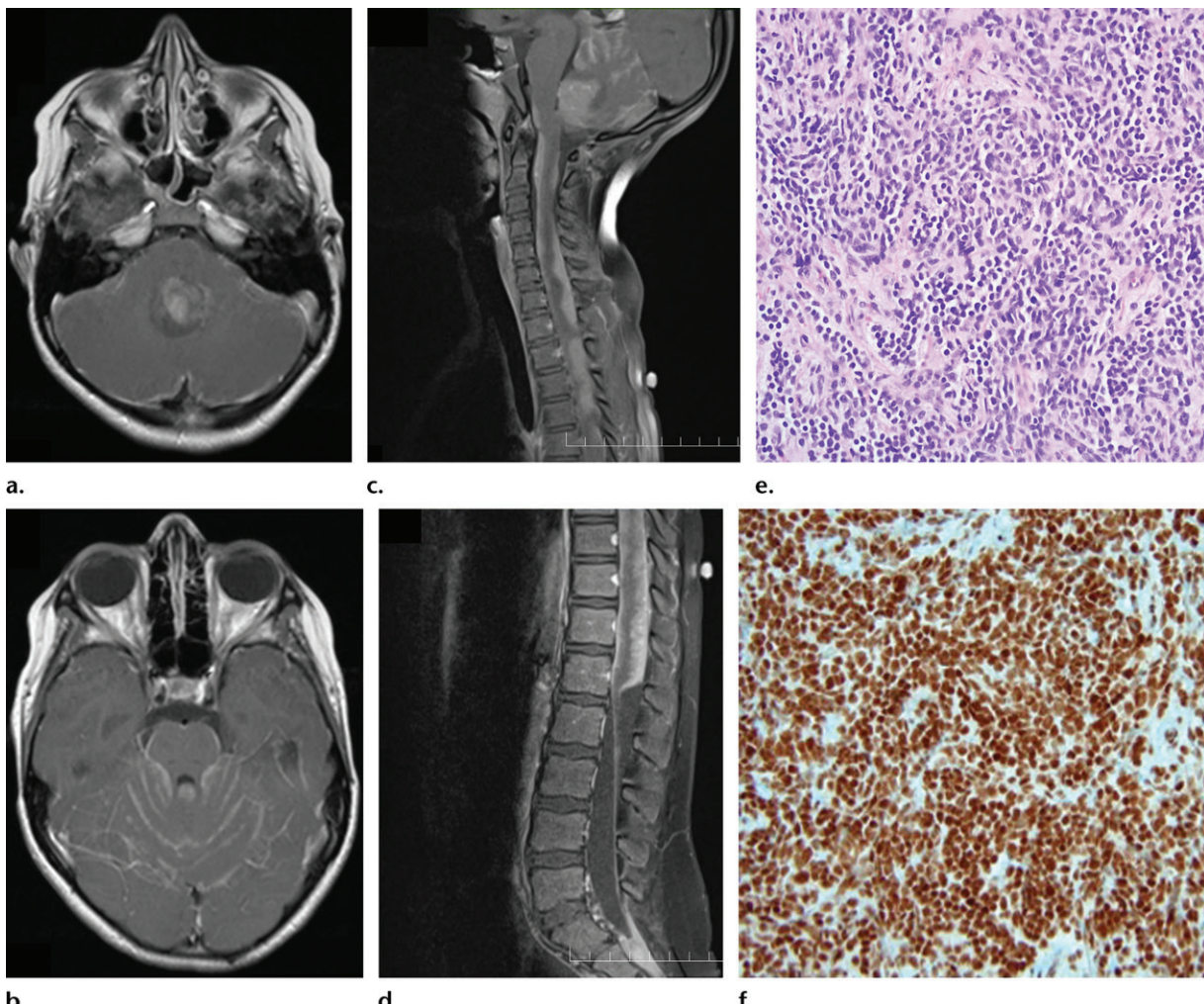


**Figure 5.** Medulloblastoma, classic (histologically defined), with CSF dissemination (drop metastasis) in an 8-year-old patient with chest/back pain, constant headache, and vomiting for 12 days. (a) Axial postcontrast T1-weighted image shows a partially enhancing mass in the midline posterior fossa. (b-d) Additional postcontrast T1-weighted images of the superior vermis and screening spine reveal abnormal leptomeningeal enhancement in the cerebellar sulci, with disseminated enhancing mass lesions along the surface of the spinal cord and at the bottom of the thecal sac. (e) Low-power photomicrograph shows sheets of densely packed undifferentiated cells with high nuclear-to-cytoplasm (N/C) ratios and focal anaplastic features. (H-E stain.) (f) Low-power photomicrograph from *BAF47/INI1* immunohistochemistry shows normal nuclear expression/positivity in the tumor cells (brown staining), which is needed to exclude a diagnosis of AT/RT. Screening for CSF dissemination should be part of the evaluation in medulloblastoma and can be positive in up to one-third of cases.

### Atypical Teratoid/Rhabdoid Tumor

A new pediatric brain tumor was first described by Lefkowitz et al in 1987 in an abstract titled “Atypical Teratoid Tumor of Infancy” because of its histologic appearance, containing an unusual mixture of primitive neuroepithelial, surface epithelial, and mesenchymal elements (52). These tumors also contained varying amounts of rhabdoid cells—which have an eccentric round nucleus with a plump cell body—similar to malignant rhabdoid tumors of infancy outside the CNS (eg, the kidney). In 1996, this entity was officially named *atypical teratoid/rhabdoid tumor*, then entered the WHO classification 4 years later (53). Because of the primitive neuroepithelial elements, many cases had probably been misdiagnosed as medulloblastoma/PNET in the past. Both are malignant

WHO grade IV embryonal tumors with a high rate of CSF dissemination in up to one-third of cases. Unlike medulloblastoma, AT/RT is often a diagnosis of infancy not childhood (median age, 17 months), is found outside the cerebellum in at least one-third of cases, and is less likely to respond to treatment (54).

Another characteristic feature of AT/RT was deletion in chromosome 22 at cytogenetic analysis. This has since been localized to the *SMARCB1* tumor suppressor gene at 22q11.2 (aliases include *BAF47*, *hSNF5*, and *INI1*). The *SMARCB1* protein is a component of the SWI/SNF (switch/sucrose nonfermentable) chromatin-remodeling complex, which regulates cell division and differentiation in normal tissues. Loss of this *SMARCB1/INI1* expression is the genetic or

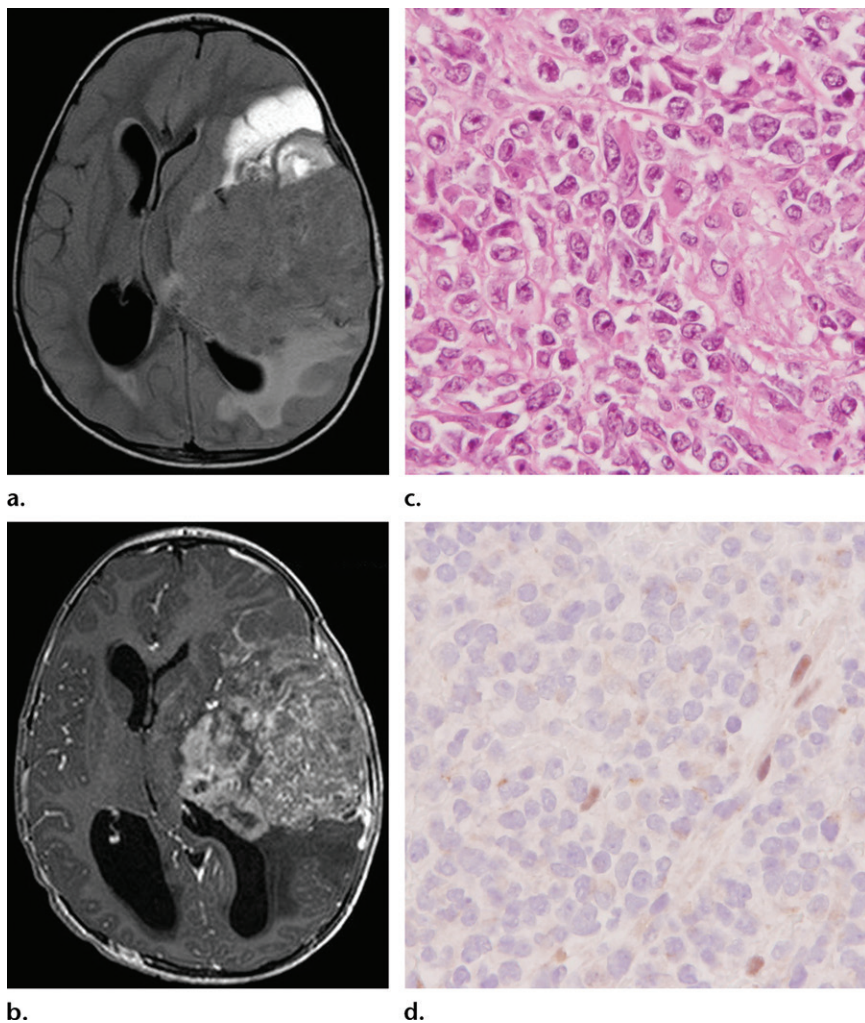


**Figure 6.** AT/RT in a 2-year-old boy with lethargy, failure to thrive, and difficulty ambulating for 2 weeks. **(a, b)** Axial T2-weighted fluid-attenuated inversion-recovery (FLAIR) **(a)** and postcontrast T1-weighted **(b)** images show a large enhancing T2-hypointense mass, with nonenhancing cysts anteriorly and vasogenic edema posteriorly, which is centered in the left cerebral hemisphere and causes subfalcine herniation with obstructive hydrocephalus. **(c)** High-power photomicrograph shows hypercellularity, correlating with the T2 hypointensity, and pleomorphic differentiation (teratoid appearance), with a few rhabdoid cells demonstrating a plump eosinophilic cytoplasm (like a pink “beer belly”) and an eccentrically placed nucleus. (H-E stain.) **(d)** High-power photomicrograph from *INI1* immunohistochemistry shows diffuse loss of nuclear expression/positivity in the tumor cells (compare with Fig 5f). There is retained staining (brown nuclei) in normal endothelial cells, which serve as a positive control. This finding is diagnostic of AT/RT.

molecular hallmark of AT/RT and is more reliable than histologic analysis for distinction from other poorly differentiated brain tumors of infancy such as choroid plexus carcinoma (55) (Fig 6). In rare cases (2%), *SMARCB1/INI1* expression is normal or retained because a different subunit of the SWI/SNF complex is inactivated (eg, *SMARCA4/BRG1* on chromosome 19p13.2) (56). In rhabdoid tumor predisposition syndrome, an inherited germline mutation in the *SMARCB1* or *SMARCA4* tumor suppressor gene puts a patient at higher risk of developing AT/RT or malignant rhabdoid tumors outside the CNS, in accordance with Knudson’s two-hit hypothesis (57).

At neuroimaging, AT/RT should be considered for any hypercellular and heterogeneous tumor of the CNS in the pediatric population, especially those under 4 years of age (>80% of cases), although adults over 20 years of age can be affected too (<2% of cases) (58). In addition to the midline or lateral posterior fossa like the more common medulloblastomas (Fig 7), they can also be found in the supratentorial compartment or spine (59). While they usually

manifest as intra-axial masses, there are rare case reports of extradural invasion of the overlying calvaria (60), tumors arising from the oculomotor nerve (61), and even primary diffuse cerebral leptomeningeal AT/RT with plaque-like disease (62) (Fig 8).

They are characterized by striking heterogeneity at CT and MR imaging, paralleling their appearance at histologic examination (hence “teratoid”) (63), often with internal calcification, hemorrhage, or cystic/necrotic changes, while displaying variable amounts of solid intratumoral enhancement and peritumoral vasogenic edema (64). Heterogeneity or variability in signal intensity and enhancement is typical of AT/RT, with evidence of leptomeningeal dissemination at initial presentation in approximately one-fourth of cases (64). The differential diagnosis includes other embryonal tumors (eg, medulloblastoma when located in the posterior fossa) and other aggressive poorly differentiated tumors of infancy (eg, immature intracranial teratoma, choroid plexus carcinoma, or rarely pediatric glioblastoma).

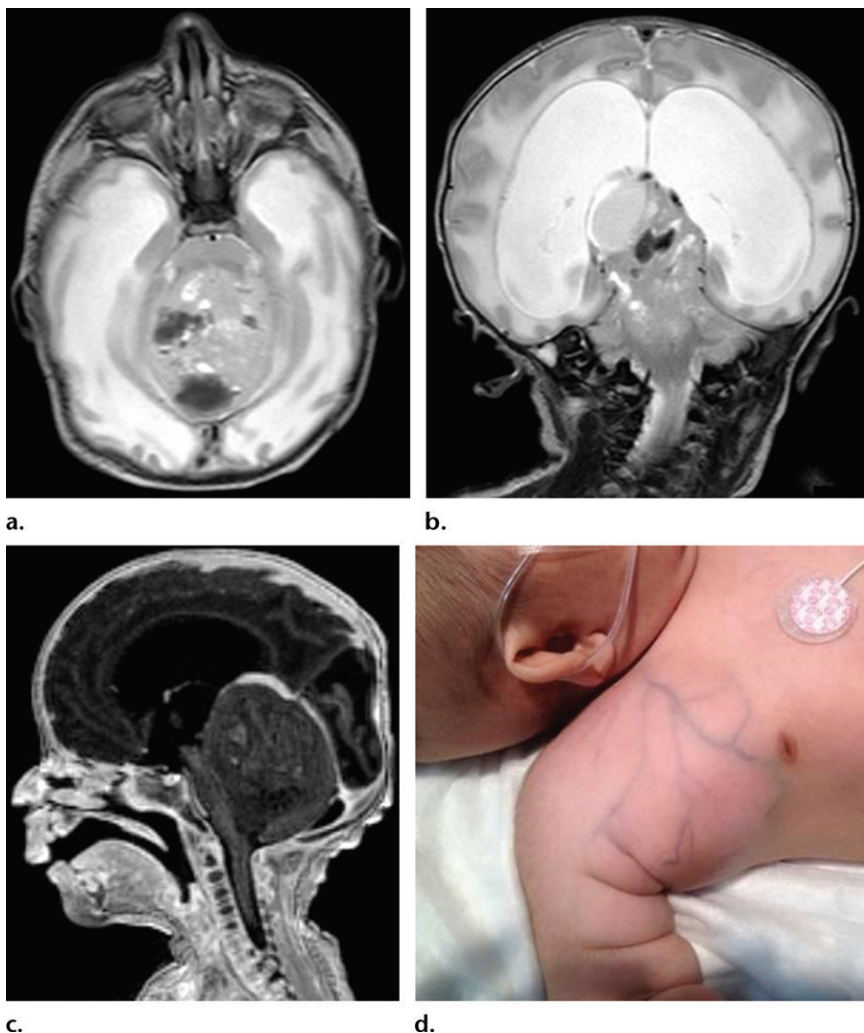


**Figure 7.** AT/RT in a male newborn with a posterior fossa mass causing obstructive hydrocephalus diagnosed with prenatal ultrasonography. (a, b) Axial (a) and coronal (b) T2-weighted images show a large midline cerebellar mass with solid, cystic, and hemorrhagic components that extends superiorly through the tentorial hiatus. (c) Sagittal postcontrast T1-weighted image shows minimal tumor enhancement and lateral-to-third ventriculomegaly. The patient's young age and tumor heterogeneity were suspicious for AT/RT, which was confirmed at immunohistochemistry by loss of *INI1* expression/staining. The patient returned 4 months later with a firm enlarging right axillary mass. (d) Photograph shows the mass, which was biopsied and initially thought to represent extradural metastasis. DNA testing uncovered a germline *INI1* mutation and raised the possibility of a second primary tumor (rhabdoid tumor predisposition syndrome).

Allowing for this characteristic heterogeneity at imaging, the solid components of these tumors will often provide clues to their embryonal or hypercellular nature. At nonenhanced CT, the solid portions are usually hyperattenuating. On T2-weighted images, they are usually isointense rather than hyperintense to gray matter (65). Diffusion-weighted imaging with ADC mapping may also be useful in gauging tumor cellularity, with one study establishing a negative correlation between  $ADC_{min}$  in AT/RT and calculated cell densities on H-E slides at  $\times 200$  magnification ( $P < .05$ ) (66).

Diffusion-weighted imaging has been shown to improve preoperative differentiation of embryonal tumors from other pediatric tumors of the CNS, for both residents in training and fellowship-trained neuroradiologists (67). On the basis of the tumor ADC, another study proposed a cutoff value for embryonal tumors ( $< 0.9 \times 10^{-3} \text{ mm}^2/\text{sec}$ ) versus ependymomas ( $1.0\text{--}1.3 \times 10^{-3} \text{ mm}^2/\text{sec}$ ) and pilocytic astrocytomas ( $> 1.4 \times 10^{-3} \text{ mm}^2/\text{sec}$ ) (68). In addition to restricted diffusion ( $ADC \sim 0.6 \times 10^{-3} \text{ mm}^2/\text{sec}$ ), dynamic susceptibility contrast (DSC) perfusion imaging

of AT/RTs shows a “return to baseline” pattern, without a T1- or T2\*-dominant contrast material leakage pattern. Spectroscopy shows an aggressive metabolite pattern, with elevated choline, lipid, and lactate peaks (69–71).

In the end, AT/RT is a pathologic diagnosis, or more specifically a genetic/molecular diagnosis, defined in 98% of cases by loss of *SMARCB1/INI1* expression. The current standard of care is maximal safe resection, followed by intensive adjuvant chemotherapy (eg, sarcoma protocols), more aggressive than for medulloblastomas. Screening MR imaging of the entire neuraxis is useful for staging; leptomeningeal spread is present in 15%–30% of patients (72). Postoperative radiation therapy to the craniospinal axis improves overall survival but is often deferred because the majority of patients are less than 3 years of age, in a critical period of neurodevelopment, and therefore at risk for long-term neurocognitive sequelae. Focal radiation therapy to the tumor bed and/or high-dose chemotherapy with autologous stem cell rescue may be options in this age group (72).

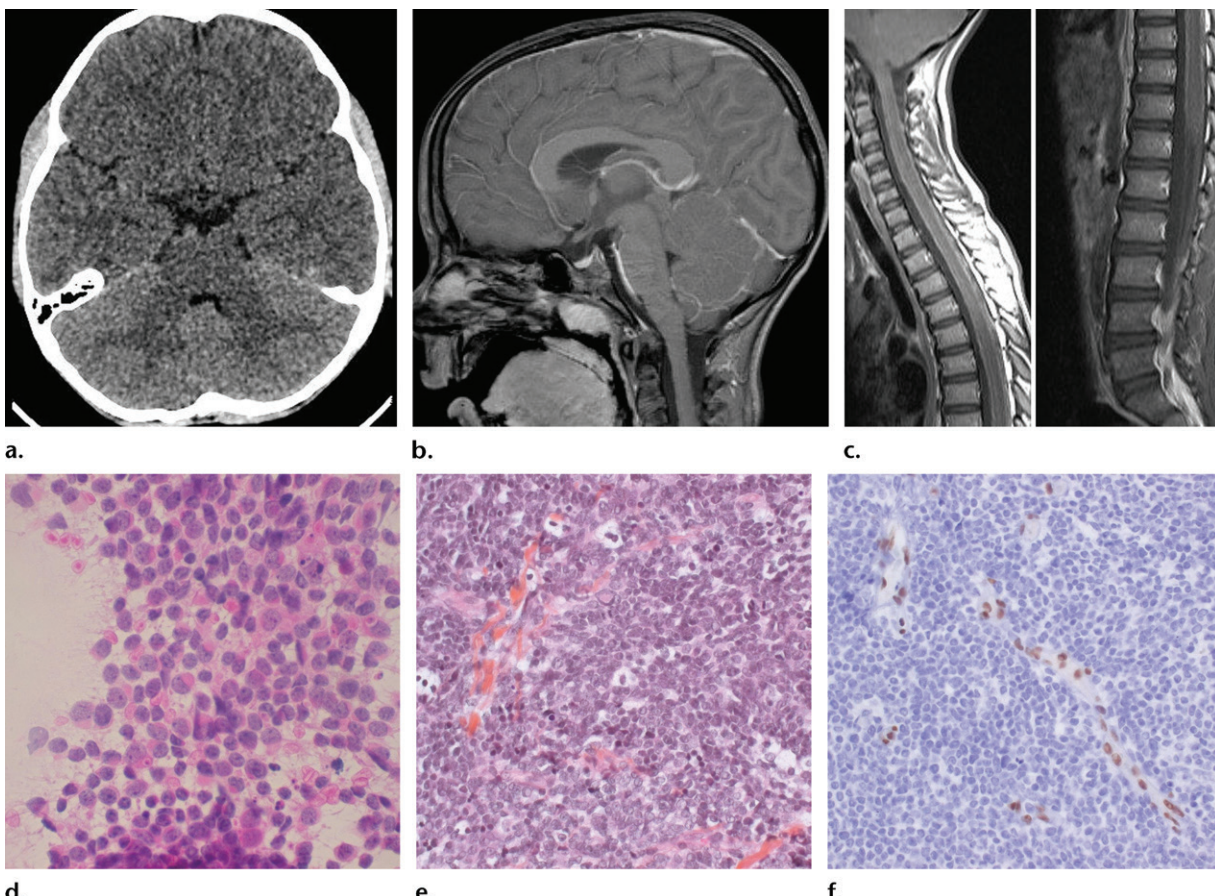


**Figure 8.** Primary leptomeningeal AT/RT in a 5-year-old boy with headaches/anorexia for 1 month and fever/emesis for 2 days. (a) Axial head CT image shows a subcentimeter hyperattenuating nodule in the right posterior suprasellar cistern, without intra-axial or parenchymal lesions. (b, c) Sagittal gadolinium-enhanced T1-weighted images of the brain (b) and spine (c) show no significant enhancement of the nodule in front of the midbrain, but do show abnormal enhancement coating the entire surface of the spinal cord, which was biopsied at the T3-T4 level. (d) Photomicrograph from intraoperative smear cytology shows a discohesive pattern with rhabdoid cells (pink cytoplasmic inclusion). (H-E stain.) (e, f) Paraffin section H-E photomicrograph (e) and photomicrograph from *INI1* immunohistochemistry (f) show a hypercellular tumor with loss of nuclear staining for *INI1*. There is retained staining (brown nuclei) in normal endothelial cells, which serve as a positive control. Primary leptomeningeal AT/RT is extremely rare but has been reported in the literature (there are four published cases).

There is variation in reported outcomes among different multimodality treatment regimens, with some long-term survivors, although in most studies the median time to relapse is less than 6 months and the median overall survival is less than 18 months (72). Nevertheless, a recent discovery that these tumors fall into three molecular subgroups (*TYR*, *SHH*, *MYC*) with different DNA methylation/expression profiles, supratentorial versus infratentorial location, and different age/gender distribution offers hope for better therapeutic targets in the future (73).

### The Tumor(s) Formerly Known as CNS PNET

At first glance, the term *primitive neuroectodermal tumor* would seem to be a synonym for any poorly differentiated or embryonal tumor of the CNS that is derived from neuroectoderm. Although it was not a founding member of the embryonal tumor category in the original 1979 WHO classification, it was

added in 1993 to account for medulloblastoma-like tumors outside the cerebellum (74). It went on to subsume the other embryonal tumors, because they were thought to be related neoplasms derived from primitive subependymal neuroepithelium, simply at different locations (eg, cerebellar PNET for medulloblastoma, pineal PNET for pineoblastoma) or in different directions of cellular differentiation at histopathologic analysis (75).

This theory fell out of favor as medulloblastomas and nonmedulloblastoma PNETs were found to differ in biology and behavior. In the 2007 WHO classification, CNS PNET “refers to a heterogeneous group of embryonal tumors... that occur at any extracerebellar site in the CNS [excluding AT/RTs]” (2). In 2016, this term was eliminated entirely.

The rise and fall of CNS PNET is a testament to the difficulty of classifying poorly differentiated tumors on the basis of histologic findings alone. Historically, diagnoses of CNS neuroblastoma,

ganglioneuroblastoma, medulloepithelioma, or ependymoblastoma reflected evidence of neuronal, ganglion cell, neural tube, or ependymal differentiation, respectively. In 2000, a new entity was described, embryonal tumor with abundant neuropil and true rosettes (ETANTR), combining histologic features from both neuroblastoma and ependymoblastoma (76).

After a case report of a high-level genomic amplification of a microRNA cluster at chromosome 19q13.42 in a 2-year-old girl with ETANTR (77), this genetic alteration was confirmed to be a sensitive and specific marker for both ETANTR and ependymoblastoma, collapsing two histologic diagnoses into a single entity (78). Another molecular feature is overexpression of *LIN28A* protein at immunohistochemistry (79), which provides a rapid inexpensive alternative to cytogenetic testing (fluorescence *in situ* hybridization [FISH]), analogous to *INI1* for AT/RT. *LIN28* proteins (*LIN28A* and *LIN28B*) are responsible for regulating and maintaining the pluripotency of embryonic stem cells by inhibiting the production of let-7 microRNA; this pathway is activated in multiple cancers.

In the 2016 WHO classification, the tumors formerly known as CNS PNET now fall mostly into one of two camps: (a) the new genetically defined entity, *ETMR, C19MC-altered*; and (b) everything else not yet genetically defined: *CNS embryonal tumor, NOS*. For the latter group, there is still the option of the historical histologically defined entities medulloepithelioma and ganglio/neuroblastoma (3).

For the former group, high-level amplification of the chromosome 19 microRNA cluster (*C19MC*) in the setting of a malignant pediatric brain tumor is unique to and diagnostic of *ETMR*, also known as group 1 CNS PNETs, replacing tumors formerly known as ependymoblastoma or ETANTR, plus many cases of medulloepithelioma (80). Most *ETMRs* arise in children younger than 4 years and in the cerebral hemispheres (81). Compared with other CNS PNETS, group 1 tumors (aka *ETMR*) manifest in younger patients (median age, 2.9 years) and show distinctly aggressive behavior (median survival, 0.8 years) (82).

At neuroimaging, the diagnosis of CNS PNET (now *ETMR* and *CNS embryonal tumor, NOS*) should be considered for any hypercellular and heterogeneous tumor of the CNS in the pediatric population, especially under 4 years of age (Fig 9). In addition to the supratentorial compartment, they can also originate in the cerebellum, brainstem, and spinal cord (83,84). Similar to AT/RTs, they are often isoattenuating to hyperattenuating and

heterogeneous at CT with internal cysts or calcifications (85). They are also hypercellular and heterogeneous at MR imaging, with isointense to hyperintense T2 signal, restricted diffusion at diffusion-weighted imaging/ADC mapping, and internal necrosis or hemorrhage (86).

*Ependymoblastoma/ETMR* specifically tends to be large with well-defined margins at presentation and also more commonly displays mild or no enhancement rather than strong enhancement (Fig 10); increased cerebral blood volume (CBV) at perfusion imaging may result from vascular endothelial hyperplasia (86). There is significant overlap in the MR imaging appearance of ependymoblastoma/ETMR and other CNS PNET/embryonal tumors, as well as high-grade supratentorial ependymoma (87). MR spectroscopy tends to show higher choline in CNS PNETs than in malignant gliomas, reflecting higher cellularity and mitotic activity (88), with elevation of taurine at 3.4 ppm, which may reflect apoptosis (89).

With regard to CNS PNETs as a group, clinical outcomes are worse than for medulloblastomas, with 5-year relative survival of 46% versus 73% based on Surveillance, Epidemiology, and End Results (SEER) data from 2000–2013 (29% for AT/RT) (5). Poor prognostic factors include CSF dissemination/metastases and either young (age < 3 years) or adult presentation; typical treatment is trimodal with maximum safe resection, adjuvant chemotherapy, and craniospinal irradiation (often withheld under 3 years of age owing to its neurotoxicity) (90). In one study of outcomes in 11 children with ependymoblastoma/ETMR registered to multicenter brain tumor trials between 1994 and 2006, there were four survivors, all of whom received craniospinal radiation therapy and/or high-dose chemotherapy with autologous stem cell rescue (91).

The transition from morphologic to molecular classification of CNS PNETs (eg, *ETMR, C19MC-altered*) will allow greater precision in clinical trials and therapeutic targets. DNA methylation profiling of 323 tumors diagnosed as CNS PNET found that 61% could be genetically reclassified as known entities, for example, high-grade glioma (31%), *ETMR* (11%), ependymoma (5%), AT/RT (4%), and medulloblastoma (3%—these were interestingly extracerebellar). Another 24% were classified as four new CNS tumor entities, while 15% did remain *CNS embryonal tumor, NOS* for now (92,93).

## Conclusion

Embryonal tumors of the CNS is a fascinating category of malignant neoplasms characterized by a predilection for the young, a propensity for

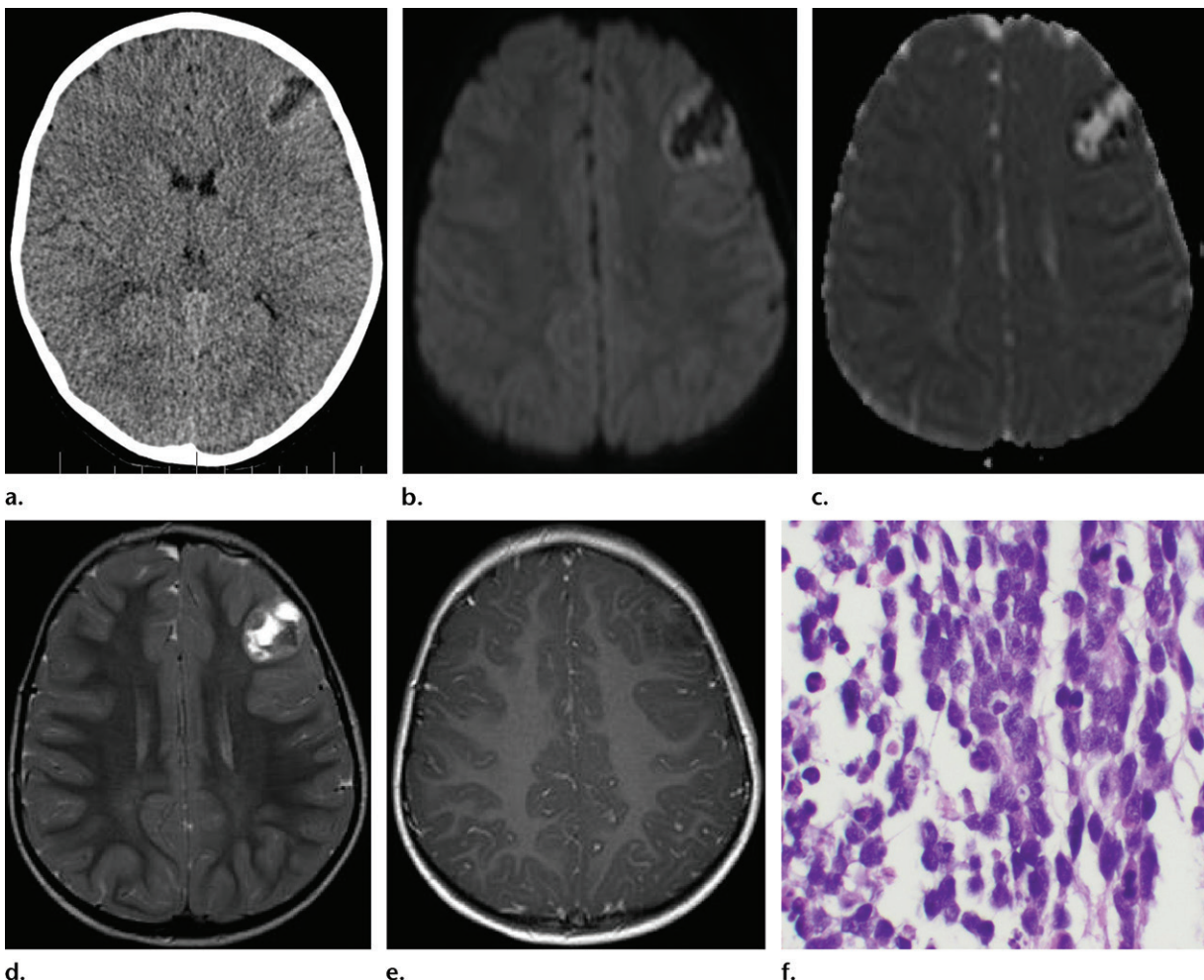


**Figure 9.** CNS PNET, which was a type of embryonal tumor in the 2007 WHO classification, in a 2-year-old boy with new-onset seizures. (a) Axial head CT image shows a peripherally hyperattenuating, centrally hypoattenuating mass at the left frontal cortex. (b, c) Axial diffusion-weighted image (b) and ADC map (c) show restricted diffusion in the periphery, suggestive of a highly cellular tumor. The differential diagnosis includes AT/RT and other nonmedulloblastoma embryonal tumors. (d, e) Axial T2-weighted (d) and postcontrast T1-weighted (e) images show a mixed solid-cystic tumor with circumscribed margins and without vasogenic edema or pathologic enhancement. (f) High-power photomicrograph shows extensive nuclear pleomorphism with both mitotic and apoptotic activity. (H&E stain.) Results of *INI1* immunostaining were positive and ruled out AT/RT. In the absence of primitive ependymal, neural tube, or neuronal/ganglion cell differentiation, the new name in the 2016 WHO classification is CNS embryonal tumor, NOS.

CSF dissemination, poorly differentiated histologic appearance (small round blue cell tumor), and high mitotic activity (Ki-67 proliferation index). Medulloblastoma accounts for nearly two-thirds of cases and is the prototypical CNS embryonal tumor of the cerebellum, with four genetically defined subtypes in the 2016 WHO classification. AT/RT and ETMR are less common and more aggressive and tend to affect the very young (age < 4 years); they are now genetically defined by loss of *INI1* expression and amplification of *C19MC*, respectively. Molecular classification is increasingly important because there is significant overlap in histologic and radiologic appearance among embryonal tumors. Their imaging features often reflect their cellularity; therefore, this category should be considered for any tumor of the CNS in a young patient with

high attenuation at CT and low signal intensity on T2-weighted images/ADC maps.

Finally, there is the question of why radiologists and radiologists-in-training should be familiar with the alphabet soup of molecular features (eg, WNT and SHH for medulloblastoma, *INI1* for AT/RT, *C19MC* or *LIN28A* for ETMR). Is it sufficient to think of and include embryonal tumor in the radiologic differential diagnosis, then wait for pathology to make the final tissue diagnosis? If the histologist may need molecular assistance to make the correct diagnosis (eg, immunohistochemical stains for protein expression or FISH analysis for chromosomal abnormalities), then what is to be expected from neuroimaging at the macroscopic level?

There are two main reasons for radiologists to be well versed in molecular terminology. The

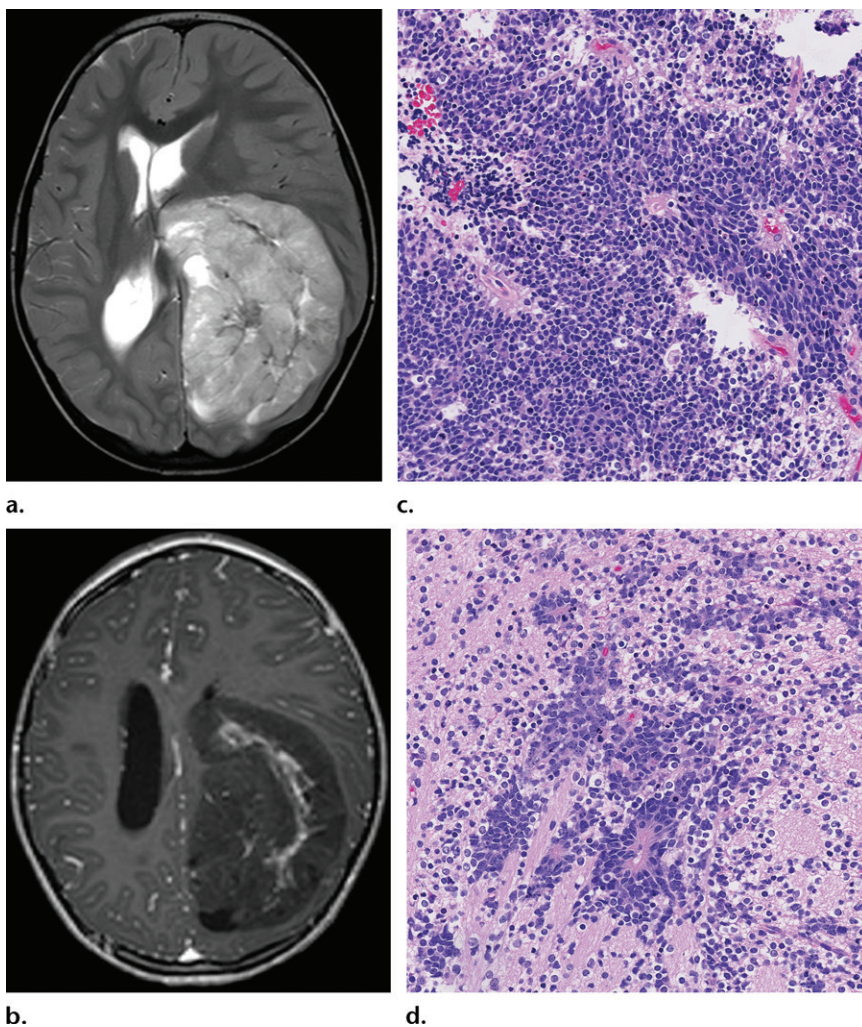


**Figure 10.** Ependymoblastoma (histologic subtype of CNS PNET in the 2007 WHO classification) in a 3-year-old girl with confusion/ataxia for 1 year and new emesis/headaches for 1 week. (a, b) Axial T2-weighted (a) and postcontrast T1-weighted (b) images show a large mildly T2 hyperintense and mildly enhancing mass in the left posterior cerebral hemisphere, with circumscribed margins and without vasogenic edema, resulting in subfalcine herniation and compressing the foramen of Monro. (c, d) Low-power photomicrographs show areas of both hypercellular sheet-like growth and paucicellular neuropil-like matrix, with a few ependymoblastic rosettes around blood vessels. (H-E stain.) The pathology report from 2010 also considered a diagnosis of ETANTR and noted genomic amplification at 19q13.42 at FISH analysis. Under the 2016 WHO classification, this would be called an ETMR, C19MC-altered.

first is to be a more effective member of the oncology team, which is eagerly transitioning into the molecular era (with or without us), moving toward better prognostic stratification and perhaps targeted therapy in the future. The second is to participate in the discovery or development of imaging patterns or methods to noninvasively predict molecular subtypes, for example, quantitative analysis of structural images (radiomics) or molecular imaging using advanced imaging techniques (eg, MR spectroscopy or PET with specialized radiotracers).

**Disclosures of Conflicts of Interest.**—K.K.K. Activities related to the present article: American Institute for Radiologic Pathology (AIRP) consulting agreement with Mayo Clinic. Activities not related to the present article: AIRP consulting agreement with Mayo Clinic. Other activities: disclosed no relevant relationships.

## References

- Scheithauer BW. Development of the WHO classification of tumors of the central nervous system: a historical perspective. *Brain Pathol* 2009;19(4):551–564.
- Louis DN, Ohgaki H, Wiestler OD, et al. The 2007 WHO classification of tumors of the central nervous system. *Acta Neuropathol (Berl)* 2007;114(2):97–109.
- Louis DN, Perry A, Reifenberger G, et al. The 2016 World Health Organization classification of tumors of the central nervous system: a summary. *Acta Neuropathol (Berl)* 2016;131(6):803–820.
- Cervoni L, Celli P, Trillo G, Caruso R. Ependymoblastoma: a clinical review. *Neurosurg Rev* 1995;18(3):189–192.
- Ostrom QT, Gittleman H, Xu J, et al. CBTRUS statistical report: primary brain and other central nervous system tumors diagnosed in the United States in 2009–2013. *Neuro Oncol* 2016;18(suppl\_5,suppl\_5):v1–v75.
- Ellison DW, Eberhart CG, Pietsch T, Pfister S. Medulloblastoma. In: Louis DN, Ohgaki H, Wiestler OD, et al, eds. WHO classification of tumors of the central nervous system. 4th ed. Lyon, France: IARC, 2016; 184–187.
- Farwell JR, Dohrmann GJ, Flannery JT. Medulloblastoma in childhood: an epidemiological study. *J Neurosurg* 1984;61(4):657–664.
- Partap S, Curran EK, Propp JM, Le GM, Sainani KL, Fisher PG. Medulloblastoma incidence has not changed over time: a CBTRUS study. *J Pediatr Hematol Oncol* 2009;31(12):970–971.
- Merchant TE, Pollack IF, Loeffler JS. Brain tumors across the age spectrum: biology, therapy, and late effects. *Semin Radiat Oncol* 2010;20(1):58–66.
- Roberts RO, Lynch CF, Jones MP, Hart MN. Medulloblastoma: a population-based study of 532 cases. *J Neuropathol Exp Neurol* 1991;50(2):134–144.
- Curran EK, Sainani KL, Le GM, Propp JM, Fisher PG. Gender affects survival for medulloblastoma only in older children and adults: a study from the Surveillance Epidemiology and End Results registry. *Pediatr Blood Cancer* 2009;52(1):60–64.

12. Yamashita Y, Handa H, Toyama M. Medulloblastoma in two brothers. *Surg Neurol* 1975;4(2):225–227.
13. Maleci A, Cervoni L, Delfini R. Medulloblastoma in children and in adults: a comparative study. *Acta Neurochir (Wien)* 1992;119(1–4):62–67.
14. Blaser SI, Harwood-Nash DC. Neuroradiology of pediatric posterior fossa medulloblastoma. *J Neurooncol* 1996;29(1):23–34.
15. Al-Mefty O, Jinkins JR, el-Senoussi M, el-Shaker M, Fox JL. Medulloblastomas: a review of modern management with a report on 75 cases. *Surg Neurol* 1985;24(6):606–624.
16. Park TS, Hoffman HJ, Hendrick EB, Humphreys RP, Becker LE. Medulloblastoma: clinical presentation and management—experience at the Hospital for Sick Children, Toronto, 1950–1980. *J Neurosurg* 1983;58(4):543–552.
17. Koeller KK, Rushing EJ. Medulloblastoma: a comprehensive review with radiologic-pathologic correlation. *RadioGraphics* 2003;23(6):1613–1637.
18. Cogen PH, McDonald JD. Tumor suppressor genes and medulloblastoma. *J Neurooncol* 1996;29(1):103–112.
19. Ellison D. Classifying the medulloblastoma: insights from morphology and molecular genetics. *Neuropathol Appl Neurobiol* 2002;28(4):257–282.
20. Ellison DW, Dalton J, Kocak M, et al. Medulloblastoma: clinicopathological correlates of SHH, WNT, and non-SHH/WNT molecular subgroups. *Acta Neuropathol (Berl)* 2011;121(3):381–396.
21. Taylor MD, Northcott PA, Korshunov A, et al. Molecular subgroups of medulloblastoma: the current consensus. *Acta Neuropathol (Berl)* 2012;123(4):465–472.
22. Eberhart CG, Giangaspero F, Ellison DW, et al. Medulloblastoma, SHH-activated. In: Louis DN, Ohgaki H, Wiestler OD, et al, eds. WHO classification of tumours of the central nervous system. 4th ed. Lyon, France: IARC, 2016; 190–192.
23. Gibson P, Tong Y, Robinson G, et al. Subtypes of medulloblastoma have distinct developmental origins. *Nature* 2010;468(7327):1095–1099.
24. Ellison DW, Giangaspero F, Eberhart CG, et al. Medulloblastoma, WNT-activated. In: Louis DN, Ohgaki H, Wiestler OD, et al, eds. WHO classification of tumours of the central nervous system. 4th ed. Lyon, France: IARC, 2016; 188–189.
25. Ellison DW, Eberhart CG, Pfister S. Medulloblastoma, non-WNT/non-SHH. In: Louis DN, Ohgaki H, Wiestler OD, et al, eds. WHO classification of tumours of the central nervous system. 4th ed. Lyon, France: IARC, 2016; 193.
26. Ryan SL, Schwalbe EC, Cole M, et al. MYC family amplification and clinical risk-factors interact to predict an extremely poor prognosis in childhood medulloblastoma. *Acta Neuropathol (Berl)* 2012;123(4):501–513.
27. Ellison DW, Eberhart CG, Giangaspero F, et al. Medulloblastoma, classic. In: Louis DN, Ohgaki H, Wiestler OD, et al, eds. WHO classification of tumours of the central nervous system. Lyon, France: IARC, 2016; 194.
28. Rutkowski S, Bode U, Deinlein F, et al. Treatment of early childhood medulloblastoma by postoperative chemotherapy alone. *N Engl J Med* 2005;352(10):978–986.
29. Pietsch T, Ellison DW, Haapasalo H, et al. Desmoplastic / nodular medulloblastoma. In: Louis DN, Ohgaki H, Wiestler OD, et al, eds. WHO classification of tumours of the central nervous system. Lyon, France: IARC, 2016; 195–197.
30. Giangaspero F, Ellison DW, Eberhart CG, et al. Medulloblastoma with extensive nodularity. In: Louis DN, Ohgaki H, Wiestler OD, et al, eds. WHO classification of tumours of the central nervous system. 4th ed. Lyon, France: IARC, 2016; 198–199.
31. Rutkowski S, von Hoff K, Emser A, et al. Survival and prognostic factors of early childhood medulloblastoma: an international meta-analysis. *J Clin Oncol* 2010;28(33):4961–4968.
32. Agrawal D, Singhal A, Hendson G, Durity FA. Gyriform differentiation in medulloblastoma: a radiological predictor of histology. *Pediatr Neurosurg* 2007;43(2):142–145.
33. Garre ML, Cama A, Bagnasco F, et al. Medulloblastoma variants: age-dependent occurrence and relation to Gorlin syndrome—a new clinical perspective. *Clin Cancer Res* 2009;15(7):2463–2471.
34. von Hoff K, Hartmann W, von Bueren AO, et al. Large cell/anaplastic medulloblastoma: outcome according to myc status, histopathological, and clinical risk factors. *Pediatr Blood Cancer* 2010;54(3):369–376.
35. Ellison DW, Giangaspero F, Eberhart CG, et al. Large cell/anaplastic medulloblastoma. In: Louis DN, Ohgaki H, Wiestler OD, et al, eds. WHO classification of tumours of the central nervous system. Lyon, France: IARC, 2016; 200.
36. Ramaswamy V, Remke M, Bouffet E, et al. Recurrence patterns across medulloblastoma subgroups: an integrated clinical and molecular analysis. *Lancet Oncol* 2013;14(12):1200–1207.
37. Loeffler JS, Kretschmar CS, Sallan SE, et al. Pre-radiation chemotherapy for infants and poor prognosis children with medulloblastoma. *Int J Radiat Oncol Biol Phys* 1988;15(1):177–181.
38. Packer RJ, Siegel KR, Sutton LN, Litmann P, Bruce DA, Schut L. Leptomeningeal dissemination of primary central nervous system tumors of childhood. *Ann Neurol* 1985;18(2):217–221.
39. Stavrou T, Dubovsky EC, Reaman GH, Goldstein AM, Vezina G. Intracranial calcifications in childhood medulloblastoma: relation to nevoid basal cell carcinoma syndrome. *AJR Am J Neuroradiol* 2000;21(4):790–794.
40. Pierce TT, Provenzale JM. Evaluation of apparent diffusion coefficient thresholds for diagnosis of medulloblastoma using diffusion-weighted imaging. *Neuroradiol J* 2014;27(1):63–74.
41. Pierce T, Kranz PG, Roth C, Leong D, Wei P, Provenzale JM. Use of apparent diffusion coefficient values for diagnosis of pediatric posterior fossa tumors. *Neuroradiol J* 2014;27(2):233–244.
42. Han C, Zhao L, Zhong S, et al. A comparison of high b-value vs standard b-value diffusion-weighted magnetic resonance imaging at 3.0 T for medulloblastomas. *Br J Radiol* 2015;88(1054):20150220.
43. Pillai S, Singhal A, Byrne AT, Dunham C, Cochrane DD, Steinbok P. Diffusion-weighted imaging and pathological correlation in pediatric medulloblastomas: “They are not always restricted!” *Childs Nerv Syst* 2011;27(9):1407–1411.
44. Yeom KW, Mobley BC, Lober RM, et al. Distinctive MRI features of pediatric medulloblastoma subtypes. *AJR Am J Roentgenol* 2013;200(4):895–903.
45. Rodriguez Gutierrez D, Awwad A, Meijer L, et al. Metrics and textural features of MRI diffusion to improve classification of pediatric posterior fossa tumors. *AJR Am J Neuroradiol* 2014;35(5):1009–1015.
46. Vicente J, Fuster-Garcia E, Tortajada S, et al. Accurate classification of childhood brain tumors by in vivo <sup>1</sup>H MRS: a multi-centre study. *Eur J Cancer* 2013;49(3):658–667.
47. Zukotynski K, Fahey F, Kocak M, et al. 18F-FDG PET and MR imaging associations across a spectrum of pediatric brain tumors: a report from the Pediatric Brain Tumor Consortium. *J Nucl Med* 2014;55(9):1473–1480.
48. Yeom KW, Mitchell LA, Lober RM, et al. Arterial spin-labeled perfusion of pediatric brain tumors. *AJR Am J Neuroradiol* 2014;35(2):395–401.
49. Li MD, Forkert ND, Kundu P, et al. Brain perfusion and diffusion abnormalities in children treated for posterior fossa brain tumors. *J Pediatr* 2017;185:173.e3–180.e3.
50. David KM, Casey AT, Hayward RD, Harkness WF, Phipps K, Wade AM. Medulloblastoma: is the 5-year survival rate improving? A review of 80 cases from a single institution. *J Neurosurg* 1997;86(1):13–21.
51. Wiener MD, Boyko OB, Friedman HS, Hockenberger B, Oakes WJ. False-positive spinal MR findings for subarachnoid spread of primary CNS tumor in postoperative pediatric patients. *AJR Am J Neuroradiol* 1990;11(6):1100–1103.
52. Bhattacharjee M, Hicks J, Langford L, et al. Central nervous system atypical teratoid/rhabdoid tumors of infancy and childhood. *Ultrastruct Pathol* 1997;21(4):369–378.
53. Rorke LB, Packer RJ, Biegel JA. Central nervous system atypical teratoid/rhabdoid tumors of infancy and childhood: definition of an entity. *J Neurosurg* 1996;85(1):56–65.
54. Burger PC, Yu IT, Tihan T, et al. Atypical teratoid/rhabdoid tumor of the central nervous system: a highly malignant tumor of infancy and childhood frequently mistaken for

- medulloblastoma—a Pediatric Oncology Group study. *Am J Surg Pathol* 1998;22(9):1083–1092.
55. Judkins AR, Burger PC, Hamilton RL, et al. INI1 protein expression distinguishes atypical teratoid/rhabdoid tumor from choroid plexus carcinoma. *J Neuropathol Exp Neurol* 2005;64(5):391–397.
  56. Hasselblatt M, Gesk S, Oyen F, et al. Nonsense mutation and inactivation of SMARCA4 (BRG1) in an atypical teratoid/rhabdoid tumor showing retained SMARCB1 (INI1) expression. *Am J Surg Pathol* 2011;35(6):933–935.
  57. Harris TJ, Donahue JE, Shur N, Tung GA. Case 168: rhabdoid predisposition syndrome—familial cancer syndromes in children. *Radiology* 2011;259(1):298–302.
  58. Lau CS, Mahendraraj K, Chamberlain RS. Atypical teratoid rhabdoid tumors: a population-based clinical outcomes study involving 174 patients from the Surveillance, Epidemiology, and End Results database (1973–2010). *Cancer Manag Res* 2015;7:301–309.
  59. Moeller KK, Coventry S, Jernigan S, Moriarty TM. Atypical teratoid/rhabdoid tumor of the spine. *AJR Am J Neuroradiol* 2007;28(3):593–595.
  60. Warmuth-Metz M, Bison B, Gerber NU, Pietsch T, Hasselblatt M, Frühwald MC. Bone involvement in atypical teratoid/rhabdoid tumors of the CNS. *AJR Am J Neuroradiol* 2013;34(10):2039–2042.
  61. Oh CC, Orr BA, Bernardi B, et al. Atypical teratoid/rhabdoid tumor (ATRT) arising from the 3rd cranial nerve in infants: a clinical-radiological entity? *J Neurooncol* 2015;124(2):175–183.
  62. El-Nabbout B, Shbarou R, Glasier CM, Saad AG. Primary diffuse cerebellar leptomeningeal atypical teratoid/rhabdoid tumor: report of the first case. *J Neurooncol* 2010;98(3):431–434.
  63. Arslanoglu A, Aygun N, Tekhtani D, et al. Imaging findings of CNS atypical teratoid/rhabdoid tumors. *AJR Am J Neuroradiol* 2004;25(3):476–480.
  64. Meyers SP, Khademian ZP, Biegel JA, Chuang SH, Kornes DN, Zimmerman RA. Primary intracranial atypical teratoid/rhabdoid tumors of infancy and childhood: MRI features and patient outcomes. *AJR Am J Neuroradiol* 2006;27(5):962–971.
  65. Cheng YC, Lirng JF, Chang FC, et al. Neuroradiological findings in atypical teratoid/rhabdoid tumor of the central nervous system. *Acta Radiol* 2005;46(1):89–96.
  66. Koral K, Mathis D, Gimi B, et al. Common pediatric cerebellar tumors: correlation between cell densities and apparent diffusion coefficient metrics. *Radiology* 2013;268(2):532–537.
  67. Koral K, Zhang S, Gargan L, et al. Diffusion MRI improves the accuracy of preoperative diagnosis of common pediatric cerebellar tumors among reviewers with different experience levels. *AJR Am J Neuroradiol* 2013;34(12):2360–2365.
  68. Rumboldt Z, Camacho DL, Lake D, Welsh CT, Castillo M. Apparent diffusion coefficients for differentiation of cerebellar tumors in children. *AJR Am J Neuroradiol* 2006;27(6):1362–1369.
  69. Kralik SF, Taha A, Kamer AP, Cardinal JS, Seltman TA, Ho CY. Diffusion imaging for tumor grading of supratentorial brain tumors in the first year of life. *AJR Am J Neuroradiol* 2014;35(4):815–823.
  70. Ho CY, Cardinal JS, Kamer AP, Lin C, Kralik SF. Contrast leakage patterns from dynamic susceptibility contrast perfusion MRI in the grading of primary pediatric brain tumors. *AJR Am J Neuroradiol* 2016;37(3):544–551.
  71. Plaza MJ, Borja MJ, Altman N, Saigal G. Conventional and advanced MRI features of pediatric intracranial tumors: posterior fossa and suprasellar tumors. *AJR Am J Roentgenol* 2013;200(5):1115–1124.
  72. Biswas A, Kashyap L, Kakkar A, Sarkar C, Julka PK. Atypical teratoid/rhabdoid tumors: challenges and search for solutions. *Cancer Manag Res* 2016;8:115–125.
  73. Johann PD, Erkek S, Zapata M, et al. Atypical teratoid/rhabdoid tumors are comprised of three epigenetic subgroups with distinct enhancer landscapes. *Cancer Cell* 2016;29(3):379–393.
  74. Kleihues P, Burger PC, Scheithauer BW. The new WHO classification of brain tumors. *Brain Pathol* 1993;3(3):255–268.
  75. Rorke LB. The cerebellar medulloblastoma and its relationship to primitive neuroectodermal tumors. *J Neuropathol Exp Neurol* 1983;42(1):1–15.
  76. Eberhart CG, Brat DJ, Cohen KJ, Burger PC. Pediatric neuroblastic brain tumors containing abundant neuropil and true rosettes. *Pediatr Dev Pathol* 2000;3(4):346–352.
  77. Pfister S, Remke M, Castoldi M, et al. Novel genomic amplification targeting the microRNA cluster at 19q13.42 in a pediatric embryonal tumor with abundant neuropil and true rosettes. *Acta Neuropathol (Berl)* 2009;117(4):457–464.
  78. Korshunov A, Remke M, Gessi M, et al. Focal genomic amplification at 19q13.42 comprises a powerful diagnostic marker for embryonal tumors with ependymoblastic rosettes. *Acta Neuropathol (Berl)* 2010;120(2):253–260.
  79. Korshunov A, Ryzhova M, Jones DT, et al. LIN28A immunoreactivity is a potent diagnostic marker of embryonal tumor with multilayered rosettes (ETMR). *Acta Neuropathol (Berl)* 2012;124(6):875–881.
  80. Spence T, Sin-Chan P, Picard D, et al. CNS-PNETs with C19MC amplification and/or LIN28 expression comprise a distinct histogenetic diagnostic and therapeutic entity. *Acta Neuropathol (Berl)* 2014;128(2):291–303.
  81. Wesseling P. Embryonal tumor with multilayered rosettes (ETMR): signed, sealed, delivered.... *Acta Neuropathol (Berl)* 2014;128(2):305–308.
  82. Picard D, Miller S, Hawkins CE, et al. Markers of survival and metastatic potential in childhood CNS primitive neuroectodermal brain tumors: an integrative genomic analysis. *Lancet Oncol* 2012;13(8):838–848.
  83. Zagzag D, Miller DC, Knopp E, et al. Primitive neuroectodermal tumors of the brainstem: investigation of seven cases. *Pediatrics* 2000;106(5):1045–1053.
  84. Benesch M, Sperl D, von Bueren AO, et al. Primary central nervous system primitive neuroectodermal tumors (CNS-PNETs) of the spinal cord in children: four cases from the German HIT database with a critical review of the literature. *J Neurooncol* 2011;104(1):279–286.
  85. Altman N, Fitz CR, Chuang S, Harwood-Nash D, Cotter C, Armstrong D. Radiologic characteristics of primitive neuroectodermal tumors in children. *AJR Am J Neuroradiol* 1985;6(1):15–18.
  86. Nowak J, Seidel C, Berg F, et al. MRI characteristics of ependymoblastoma: results from 22 centrally reviewed cases. *AJR Am J Neuroradiol* 2014;35(10):1996–2001.
  87. Nowak J, Seidel C, Pietsch T, et al. Systematic comparison of MRI findings in pediatric ependymoblastoma with ependymoma and CNS primitive neuroectodermal tumor not otherwise specified. *Neuro Oncol* 2015;17(8):1157–1165.
  88. Majos C, Alonso J, Aguilera C, et al. Adult primitive neuroectodermal tumor: proton MR spectroscopic findings with possible application for differential diagnosis. *Radiology* 2002;225(2):556–566.
  89. Kovanlikaya A, Panigrahy A, Krieger MD, et al. Untreated pediatric primitive neuroectodermal tumor *in vivo*: quantitation of taurine with MR spectroscopy. *Radiology* 2005;236(3):1020–1025.
  90. Lester RA, Brown LC, Eckel LJ, et al. Clinical outcomes of children and adults with central nervous system primitive neuroectodermal tumor. *J Neurooncol* 2014;120(2):371–379.
  91. Gerber NU, von Hoff K, von Bueren AO, et al. Outcome of 11 children with ependymoblastoma treated within the prospective HIT-trials between 1991 and 2006. *J Neurooncol* 2011;102(3):459–469.
  92. Sturm D, Orr BA, Toprak UH, et al. New brain tumor entities emerge from molecular classification of CNS-PNETs. *Cell* 2016;164(5):1060–1072.
  93. Zaky W. Revisiting management of pediatric brain tumors with new molecular insights. *Cell* 2016;164(5):844–846.